Gate-Dependent Magnetoresistance Phenomena in Carbon Nanotubes

G. Fedorov, B. Lassagne, M. Sagnes, B. Raquet, and J.-M. Broto

Laboratoire National des Champs Magnetiques Pulsés, UMR5147, 143 avenue de rangueil, 31342 Toulouse, France

F. Triozon and S. Roche

Commissariat à l'Energie Atomique, DSM/DRFMC/SPSMS and DRT/LETI/D2NT/LSCP, 17 rue des Martyrs, 38054 Grenoble, Cedex 9 France

E. Flahaut

Centre Inter universitaire de Recherche et d'Ingénierie des MATériaux-UMR CNRS 5085-Université Paul Sabatier, 31062 Toulouse, Cedex 04 France

(Received 2 July 2004; published 14 February 2005)

We report on the first experimental study of the magnetoresistance of double-walled carbon nanotubes under a magnetic field as large as 50 T. By varying the field orientation with respect to the tube axis, or by gate-mediated shifting the Fermi level position, evidence for unconventional magnetoresistance is presented and interpreted by means of theoretical calculations.

DOI: 10.1103/PhysRevLett.94.066801 PACS numbers: 73.63.Fg, 72.15.Rn

Since their discovery, carbon nanotubes have been the focus of numerous studies, and intense debate has been carried out concerning the nature of their electronic transport properties. The initial prediction of their electronic properties [1] and the possibility to obtain ideal 1D-ballistic conductors [2] have been confirmed experimentally by means of the scanning tunneling microscopies [3] or transport measurements of nanotube-based devices [4].

More precisely, depending on their helical symmetries, the electronic properties manifest either a metallic or a semiconducting character. The origin of such behavior comes from the distribution of available states in the reciprocal space, as a consequence of quantization conditions (in relation with the circumference of the tube, and periodic boundary conditions), and in function of symmetry considerations. The application of a magnetic field is able to modulate the distribution of such states, resulting in strong modifications of the electronic spectrum [5]. Recently, such prediction of Aharonov-Bohm effects on the density of states was challenged experimentally on both large multiwalled nanotubes in the Coulomb blockade regime [6] and on single-walled nanotubes (SWNTs) by magneto-optical spectroscopy [7].

On the other side, while the first magnetotransport experiments performed on large diameter multiwalled nanotubes have clearly evidenced signatures of weak localization (WL) phenomena with negative magnetoresistance effects and $\phi_0/2$-periodic Aharonov-Bohm oscillations [8], works of others have proposed contradictory interpretations of magnetotransport data [9] as mainly stemming from the magnetic dependence of the density of states (DOS) of a clean system in the ballistic regime [9]. To unravel the possible competing contributions enclosed within magnetofingerprints, it has been theoretically proposed to explore the gate-dependent variations of the magnetoresistance patterns [10]. A gate-dependent magnetotransport study at low field has recently enabled one to discuss the Luttinger liquid scenario in multiwalled nanotubes [11].

In this Letter, the magnetoresistance of double-walled carbon nanotubes with a 3 nm diameter is investigated in large magnetic field up to 50 T, and as a function of applied gate voltage, temperature, and magnetic-field orientation with respect to the tube axis. Unconventional fingerprints are unveiled such as a switching mechanism from negative to positive magnetoresistance as a function of applied gate voltage. The analysis of the experimental data is consistent with the scenario of a strong contribution from the magnetic-field modulated density of states in conjunction with weak localization effects. The numerical computation of the Landauer-Büttiker magnetoconductance also confirms such a phenomenon, and a consistent theoretical explanation of experiments is proposed assuming an initial up-shift of the Fermi level with respect to the charge neutrality point, attributed to unavoidable doping from the contacts or contaminants.

Our experiments are performed on small, 2.5 μm long, bundles of double-walled nanotubes (DWNTs) deposited on the tops of two gold nanoelectrodes, and with a typical diameter of 8 nm (the bundle contains thus less than nine nanotubes). The synthesis of DWNTs by chemical vapor deposition and the nanomanipulation for positioning the bundles have been presented elsewhere [12–14].

The individual DWNTs present a well defined diameter, centered around 1–3 nm. Given the expected proportion of metallic tubes (1/3), and owing to some device geometry considerations, electronic transport should be statistically dominated by a single metallic tube. This statement seems to be consistent with our (magneto)transport data as detailed hereafter.

First, at zero magnetic field, the two probe resistance is typically on the order of 150 kΩ at room temperature, and it increases with lowering the temperature to reach 550 kΩ at 2 K, for a 50 mV applied bias voltage. The differential conductance $G = dI/dV$ exhibits a zero bias anomaly (ZBA) which is markedly enhanced at low temperatures (Fig. 1). Whereas the appearance of ZBA and a power law behavior of $G(T, V_b)$ is usually interpreted in terms of Luttinger liquid (LL) behavior for SWNT [15], the situation is more controversial for multiwalled nanotubes (MWNTs) since LL-like ZBA can also be achieved from other considerations [11,16]. In our experiment, gate effects on the differential conductance $G(V_G)$ exhibit relevant structures depending on the temperature and the bias voltage (inset of Fig. 1). For small bias voltage, small modulations of $G(V_G)$ already appear at 80 K, where charging effects are excluded. This seemingly suggests some energy dependent structures of the DOS. Indeed, electronic resonant backscattering on quasibound states due to structural defects and/or impurities along the tube are known to modify the local DOS close to the charge neutrality point [17].

The impact of large magnetic fields on the transport properties is studied in the high kinetic energy regime: the voltage drop across the sample is fixed well above the ZBA as shown by the arrow in Fig. 1, for experiments at 4 K. In this regime, it is likely that the measured field dependence of the conductance is an intrinsic property of the tube. For small polarization, within the ZBA, the total resistance is widely dominated by the tunnel resistance at the contacts and measurements of the magnetoconductance (MC) give a negligible field dependence whatever the gate voltage.

Figure 2 shows the conductance variation $\Delta G(B) = G(B) - G(0)$ at 80 K for magnetic fields parallel ($B_{\|}$) and perpendicular ($B_{\perp}$) to the tube.

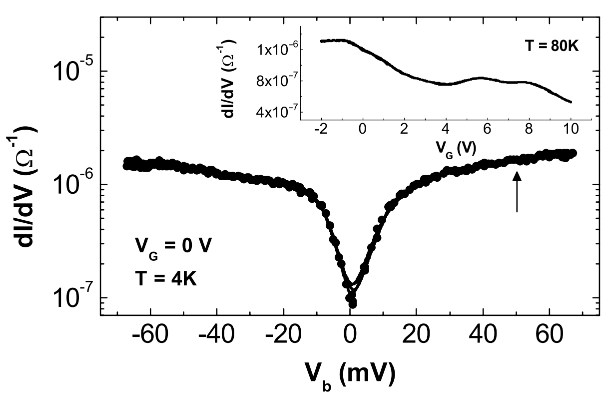

FIG. 1. Differential conductance vs applied bias voltage at 4 K for $V_G = 0$ V. The arrow indicates the high energy regime studied under 50 T at 4 K. In the inset, the gate voltage effects on the differential conductance for $V_b = 20$ mV at 80 K.

In both cases, the applied field increases the conductance of the NT, and the saturation is almost reached below 50 T. The corresponding MC is, respectively, 10% and 6% at 50 T for $B_{\|}$ and $B_{\perp}$, whereas minor gate voltage dependences are observed on $\Delta G(B)$ at this temperature.

The origin of the positive MC is elaborated in terms of a field induced dephasing effect of the electron wave interference in the WL regime. Indeed, let us consider a hollow cylinder of diameter $2R = 2.8$ nm with a wall thickness $a = 0.14$ nm. Based on Altshuler-Aronov-Spivak (AAS) calculations [18], the conductance variation $\Delta G_{\mathrm{WL}}(B)$ as a function of a magnetic field applied along the tube axis can be expressed as follows:

$$\Delta G_{\mathrm{WL}}(B) = -A\frac{e^2}{\pi\hbar}\frac{2\pi R}{L}\left\{\ln\left(\frac{L_\varphi(B)}{L}\right) + 2\sum_n\left[K_0\left(\frac{n2\pi R}{L_\varphi(B)}\right)\right.\right.$$
$$\left.\left.\times\cos\left(2\pi n\frac{2\phi}{\phi_0}\right) - K_0\left(\frac{n2\pi R}{L_\varphi}\right)\right]\right\}, \qquad (1)$$

where $K_0(x)$ is the Macdonald function and $\phi = \pi R^2 B$. $L_\varphi(B)$ is the phase coherence length defined by $1/L_\varphi^2(B) = 1/L_\varphi^2 + (WeB/\hbar)^2/3$, where L_φ is the phase coherence length at zero field and $W = a$ (the wall thickness) in parallel configuration. The A factor accounts for the contact transparency of the interface in the two probe measurements. Using Eq. (1) with two fitting parameters (L_φ and A), a convincing agreement (solid line, Fig. 2) to the experimental data for $B_{\|}$ is obtained from zero to 50 T, with L_φ equal to 30 nm at 80 K and $A \simeq 0.7$. Extrapolation to very high field shows that the WL contribution is already strongly reduced at 50 T, whereas AAS oscillations with a $\phi_0/2$ period corresponding to 336 T are expected (inset of

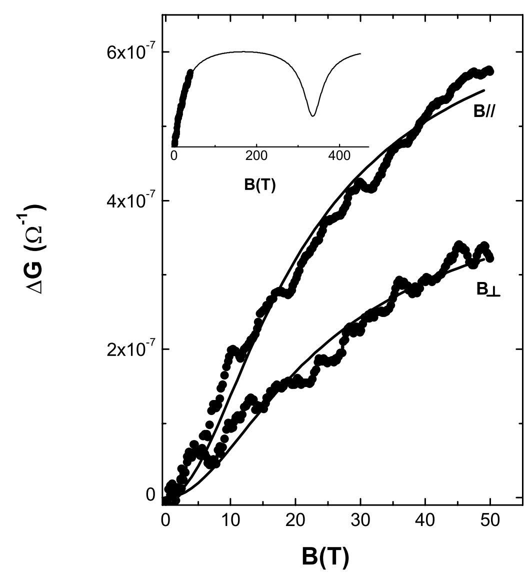

FIG. 2. Magnetoconductance $\Delta G(B)$ up to 50 T for $B_{\|}$ and $B_{\perp}$ with a bias voltage $V_b = 300$ mV and zero gate voltage at 80 K. Solid lines represent the quasi-2D WL fits for both configurations. Inset: the predicted $\Delta G(B_{\|})$ from Eq. (1) in a very high field, superimposed to our measurement.

Fig. 2). Note that the A value corresponds to rather transparent contacts in the high bias voltage regime. The same value is used to fit all the data at other temperatures for both $B_{\parallel}$ and $B_{\perp}$.

Equation (1) is easily rewritten in the $B_{\perp}$ case considering the surface of the tube perpendicular to the field. The field dependence of the phase coherence length varies within the diameter of the tube instead of the wall thickness for the parallel case. For a width $W \approx 2R$ and $\phi = 0$, we straightforwardly derive a new expression for $\Delta G_{\mathrm{WL}}(B)$, which yields very good agreement with our data in the perpendicular configuration with $L_{\varphi} \approx 28$ nm (solid line, Fig. 2). The consistency between $B_{\parallel}$ and $B_{\perp}$ up to 50 T clearly demonstrates that quantum interferences in the WL regime dominate the DWNT conductivity at 80 K with a phase coherence length a few times larger than the circumference.

The situation at 4.2 K gains in complexity. From here on, we focus on the $B_{\parallel}$ case. At zero gate voltage, a positive MC is observed up to $B \approx 7$ T, above which a large negative MC dominates with no hint of saturation (Fig. 3, left panel). Applying a 10 V gate voltage astonishingly suppresses the high negative MC, and $\Delta G(B)$ remains positive with no sign of saturation up to 50 T. The electrostatic doping under 50 T tunes the MC from negative (-10%) to positive ($+35\%$). Changes of MC for different V_G are detailed in Fig. 3, right panel. An increase of the gate voltage gradually decreases the low field positive MC. Simultaneously, the high field MC changes from a negative sloop to a positive one.

These unconventional magnetofingerprints cannot be strictly interpreted from quantum interference effects. The nonmonotonic MC in $B_{\parallel}$, at 4 K, and zero gate voltage, clearly results from the superposition of a very sensitive positive MC in low field and a large negative MC which dominates the high field regime. A likely origin of the low field positive MC is, once again, WL around the circumference of the tube. Fitting the low field MC with Eq. (1) and $L_{\varphi}(4\ \mathrm{K})$ as a unique parameter gives reasonable agreement with a phase coherence length equal to 84 nm (solid line, inset of Fig. 3, left panel). The ratio $L_{\varphi}(78\ \mathrm{K})/L_{\varphi}(4\ \mathrm{K})$ agrees remarkably well with a $T^{-1/3}$ dependence, a fact consistent with a dephasing by quasielastic electron-electron scattering [18].

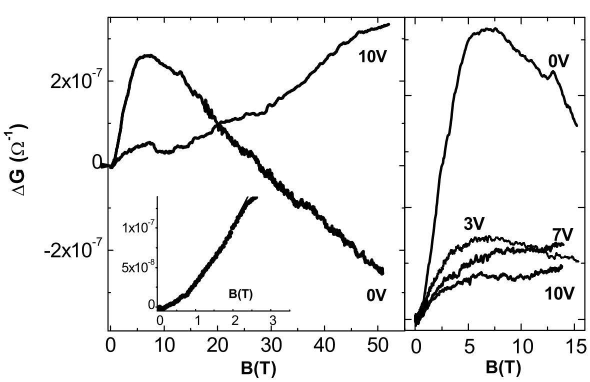

FIG. 3. Left panel: Magnetoconductance $\Delta G(B_{\parallel})$ up to 50 T with a bias voltage $V_b = 50$ mV and for $V_G = 0$ and 10 V at 4 K. Inset: low magnetic-field fit with the quasi 2D WL model (solid line), using Eq. (1) up to $B_{\parallel} = 3$ T. Right panel: The low field variations of $\Delta G(B_{\parallel})$ for different gate voltages from 0 to 10 V.

To investigate the origin of the drastic change of MC in a high parallel field versus V_G, a numerical study of the Landauer-Büttiker conductance of a nanotube-based heterojunction is performed, using a standard procedure [19]. The whole system is made from two semi-infinite disorder-free (22, 22) metallic tubes, with diameter 3 nm, that describe the external leads, whereas the central part consists of the same metallic nanotube with length 100 nm, and in which an elastic disorder (Anderson type) together with a magnetic field are introduced. The common tight-binding Hamiltonian is used with constant integral overlap γ_0 between first neighbors, whereas site energies ε_n are randomly distributed within an interval $[-W/2, W/2]$ (uniform density) to simulate an elastic disorder. Under the application of a magnetic field, standard procedures are used to implement the Peierls phase factors contribution to the quantum phases [5,10]. In this description, a useful analytical estimation of the elastic mean free path [2] can be derived, enabling one to discriminate between ballistic and diffusive, as well as localized, regimes. Two values of disorder are chosen to make the mean free path in the vicinity of the charge neutrality point either much larger ($W = 1$, in units of γ_0) or on the order of the nanotube circumference ($W = 2$), for which the conventional weak localization framework strictly applies [8]. The main results are reported in Fig. 4 where the conductance is plotted

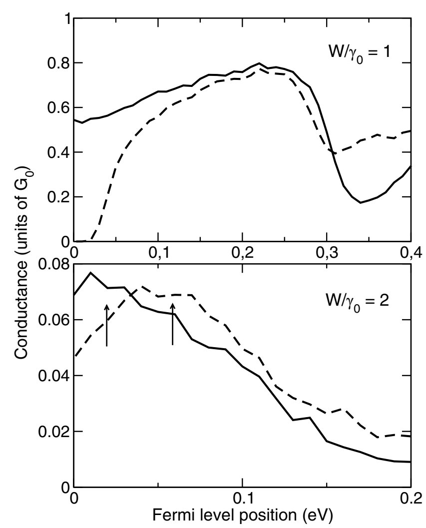

FIG. 4. Conductance versus Fermi level position, for a disordered (22, 22) nanotube, and two values of the parallel magnetic field: $B_{\parallel} = 0$ T (solid line) and $B_{\parallel} = 50$ T (dashed line). Two disorder strengths are considered: $W/\gamma_0 = 1$ (upper panel) and $W/\gamma_0 = 2$ (lower panel). In the strong disorder case, the two arrows indicate possible Fermi level positions for $V_G = 0$ V (left) and $V_G = 10$ V (right).

for two values of disorder, at zero magnetic field, and for $B_{\|} = 50$ T, to cope with the experimental range.

The quantum conductance at zero field is first found to be strongly energy dependent, in agreement with prior results [20]. One notes, in particular, that it decreases in the vicinity of the van Hove singularities due to a decrease of the relaxation time. More interesting is the role of the magnetic field that induces two competing trends. First, the WL contribution yields positive MC. For moderate disorder ($W = 1$), it dominates only within the semiconducting subbands, where the mean free path becomes of the order of the tube circumference. For sufficiently strong disorder ($W = 2$), the WL contribution is important and yields positive MC for a large part of the spectrum. Second, the magnetic field also affects the electronic structure, an effect that is more predominant in the vicinity of the charge neutrality point, given the opening of the energy pseudogap, followed by its enlargement, and resulting in a negative contribution to the MC. One may thus interpret experimental results reported in Fig. 3 at zero gate voltage as a signature of such competing contributions of quantum interferences and density of state effects which are expected to dominate in high field. A consistent interpretation of the experimental results is possible in the strong disorder case $W = 2$. An initial position of the Fermi level is proposed in Fig. 4 (left arrow). For this energy, positive MC due to WL dominates at low field (numerical result not shown here) and negative MC due to the energy pseudogap dominates at high field. The application of a positive gate voltage, by up-shifting the initial Fermi level, consistently reduces the contribution from DOS effects, and yields a positive MC as reported in Fig. 3. From the differential conductance measurements versus V_G within the ZBA [21], we estimate the back-gate capacitance C_g on the order of a few pF per meter. The expected Fermi level up-shift, given by $\Delta E_f = eV_g C_g / C_{\mathrm{NT}}$ (C_{NT} is the electrochemical capacitance) under 10 V is thus around 50 meV. Its position at $V_G = 10$ V is represented by the right arrow in Fig. 4. The reduction of the zero-field conductance at a higher gate voltage is also consistently found in theoretical and experimental results (Fig. 1). Interestingly, if one sketches the eventual contribution of an additional semiconducting tube parallel to the metallic one, one notices that its band gap reduction due to the magnetic field is much too small to affect the MC. This states that a single metallic NT is likely to account for the measured gate-dependent MC. The assumption of a diffusive regime allows us to rescale the computed zero-field conductance obtained for $W = 2$ and for tube length 100 nm. The numerical estimate for the same device but with a length of 2.5 μm gives a conductance value comparable to but slightly below the experimental measure. This may originate from the fact that the numerical calculations are performed in the fully coherent regime for a tube length of 100 nm, which is larger that the coherence length estimated experimentally ($\leq$80 nm). Finally, our gate-dependent MC measurements reveal that characteristic lengths in diffusive DWNT make possible a nontrivial coexistence between quantum interference along the circumference and electronic band structure modulation. Results are significantly different in the case of NTs in the Coulomb blockade regime [6], for which gate and magnetic-field effects give a spectroscopy of the electronic energy levels.

The authors thank Th. Ondarçuhu for experimental assistance on DWNT deposition. Substrate preparations have been performed in the LAAS technological platform. This work has been supported by the French ministry of research under program ACI "Nanosciences 2004" No. NR044 "NOCIEL." F. T. and S. R. acknowledge support from the Micro and Nanotechnology program from the French ministry of research under the grant RTB: Post CMOS moleculaire 200mm and the research grant from French ministry of research under ACI project TransNanoFils.

[1] R. Saito, G. Dresselhaus, and M. Dresselhaus, *Physical Properties of Carbon Nanotubes* (Imperial College Press, London, 1998).
[2] C. T. White and T. N. Todorov, Nature (London) **393**, 240 (1998).
[3] J. W. Wildoer *et al.*, Nature (London) **391**, 59 (1998).
[4] A. Javey *et al.*, Nature (London) **424**, 654 (2003); J. Appenzeller *et al.*, Phys. Rev. Lett. **92**, 048301 (2004).
[5] H. Ajiki and T. Ando, J. Phys. Soc. Jpn. **62**, 1255 (1993).
[6] U. C. Coskun *et al.*, Science **304**, 1132 (2004).
[7] S. Zaric *et al.*, Science **304**, 1129 (2004).
[8] L. Langer *et al.*, Phys. Rev. Lett. **76**, 479 (1996); C. Schönenberger *et al.*, Appl. Phys. A **69**, 283 (1999).
[9] A. Fujiwara *et al.*, Phys. Rev. B **60**, 13 492 (1999); J. O. Lee *et al.*, Phys. Rev. B **61**, R16 362 (2000); C. Schönenberger and A. Bachtold, Phys. Rev. B **64**, 157401 (2001); J. Kim *et al.*, Phys. Rev. B **64**, 157402 (2001).
[10] S. Roche and R. Saito, Phys. Rev. Lett. **87**, 246803 (2001).
[11] A. Kanda *et al.*, Phys. Rev. Lett. **92**, 036801 (2004).
[12] E. Flahaut *et al.*, Chem. Commun. **2003**, 1442 (2003).
[13] S. Gerdes *et al.*, Europhys. Lett. **48**, 292 (1999).
[14] M. Sagnes *et al.*, Microelectron. Eng. **67–68**, 683 (2003).
[15] M. Bockrath *et al.*, Nature (London) **397**, 598 (1999).
[16] K. Liu *et al.*, Phys. Rev. B **63**, 161404(R) (2001).
[17] H. J. Choi *et al.*, Phys. Rev. Lett. **84**, 2917 (2000).
[18] A. G. Aronov and Y. V. Sharvin, Rev. Mod. Phys. **59**, 755 (1987).
[19] S. Datta, *Electronic Transport in Mesoscopic Systems* (Cambridge University Press, Cambridge, 1997).
[20] F. Triozon *et al.*, Phys. Rev. B **69**, 121410 (2004).
[21] G. Fedorov *et al.* (to be published).